

Resonant photoemission of Ga_{1-x}Mn_xAs at the Mn *L* edge

O. Rader,* C. Pampuch, and A. M. Shikin[†]
BESSY, Albert-Einstein-Str. 15, D-12489 Berlin, Germany

W. Gudat
BESSY, Albert-Einstein-Str. 15, D-12489 Berlin, Germany
and Institut für Physik, Universität Potsdam, P.O. Box 601553, D-14415 Potsdam, Germany

J. Okabayashi, T. Mizokawa, and A. Fujimori
Department of Physics and Department of Complexity Science and Engineering, University of Tokyo, 7-3-1 Hongo, Bunkyo-ku, Tokyo 113-0033, Japan

T. Hayashi and M. Tanaka
Department of Electronic Engineering, University of Tokyo, 7-3-1 Hongo, Bunkyo-ku, Tokyo 113-8656, Japan

A. Tanaka
Department of Quantum Matter, ADSM, Hiroshima University, 1-3-1 Kagamiyama, Higashi-Hiroshima 739-8526, Japan

A. Kimura
Department of Physical Sciences, Hiroshima University, 1-3-1 Kagamiyama, Higashi-Hiroshima 739-8526, Japan

(Received 22 April 2003; revised manuscript received 6 November 2003; published 6 February 2004)

Ga_{1-x}Mn_xAs, $x = 0.043$, has been grown *ex situ* on GaAs(100) by low-temperature molecular-beam epitaxy. On the reprepared $p(1 \times 1)$ surface, resonant photoemission of the valence band shows a 20-fold enhancement of the Mn 3*d* contribution at the *L*₃ edge. The difference spectrum is similar to our previously obtained resonant photoemission at the Mn *M* edge, in particular a strong satellite appears and no clear Fermi edge ruling out strong Mn 3*d* weight at the valence-band maximum. The x-ray absorption lineshape differs from previous publications. Our calculation based on a configuration-interaction cluster model reproduces the x-ray absorption and the *L*₃ on-resonance photoemission spectrum for model parameters Δ , U_{dd} , and $(pd\sigma)$ consistent with our previous work and shows the same spectral shape on and off resonance thus rendering resonant photoemission measured at the *L*₃ edge representative of the Mn 3*d* contribution. At the same time, the results are more bulk sensitive due to a probing depth about twice as large as for photoemission at the Mn *M* edge. The confirmation of our previous results obtained at the *M* edge calls recent photoemission results into question which report the absence of the satellite and good agreement with local-density theory.

DOI: 10.1103/PhysRevB.69.075202

PACS number(s): 75.50.Pp, 79.60.Bm, 71.27.+a

I. INTRODUCTION

In the research field of diluted magnetic semiconductors, the recent observation of long-range ferromagnetic order represented a major breakthrough.¹⁻⁴ The materials that exhibit this ferromagnetic behavior are the Mn-doped III-V compounds InAs and GaAs prepared by molecular-beam epitaxy. In these materials, Mn occupies Ga or In sites of the zinc blende lattice. It is understood that the origin of ferromagnetism is connected to a twofold effect of the Mn impurities: on the one hand they provide localized magnetic moments, on the other hand they act as a hole dopant. Nevertheless, the physics of the long-range ferromagnetic interaction remains controversial, basic questions being whether this interaction is mediated by Mn 3*d*-Mn 3*d* interaction or Mn 3*d*-As 4*p* and whether the latter would couple spins parallel or antiparallel. More precise knowledge of the electronic structure of the Mn impurities in this system is therefore required.

Previously, we studied the Mn 2*p* core level by x-ray photoelectron spectroscopy and analyzed the spectrum with

its strong satellite using configuration-interaction calculations taking into consideration the local surrounding of the Mn impurity in a cluster model.⁵ The Mn *d* electron number was determined to be ≥ 5 and both Mn⁺² and Mn⁺³ states were found to be in agreement with the experimental data.⁵ The exchange constant $N\beta$ was determined as -1.2 ± 0.2 eV meaning antiferromagnetic Mn 3*d*-As 4*p* interaction in the case of the half-occupied Mn²⁺ ion. Because of the strong magnetic coupling between Mn³⁺ and an As 4*p* hole, the hole will be responsible for the long-range magnetic interaction. Valence-band photoemission⁶ at and above the Mn *M* edge (50 eV) permitted assignment of structures in the local Mn 3*d* contribution to the excitation spectrum to d^4 , $d^5\bar{L}$, and $d^6\bar{L}^2$ configurations, i.e., configurations where the number of electrons transferred from As 4*p* orbitals to Mn 3*d* is zero, one, and two, respectively. Besides a strong main peak around -4.5 eV assigned to $d^5\bar{L}$, an intense valence-band satellite was seen to be caused by d^4 plus $d^6\bar{L}^2$ contributions. The average Mn configuration was determined to be $3d^{5.3 \pm 0.1}$.

The possibility to distinguish Mn 3*d* derived states by resonant photoemission at the Mn *M* edge is particularly important for the region near the Fermi energy. Apart from intensity predicted for $d^5\bar{L}$ near -2 eV, there is almost no intensity near E_F in the spectra measured. Substantial Mn 3*d* derived intensity at E_F had been predicted by coherent-potential approximation local-density calculations for $\text{In}_{1-x}\text{Mn}_x\text{As}$ and $\text{Ga}_{1-x}\text{Mn}_x\text{As}$ in Ref. 7 with the interesting consequence that these systems would belong to the class of half metals. Angle-resolved photoemission of $\text{Ga}_{1-x}\text{Mn}_x\text{As}(100)$, $x=0.069$, showed very similar band dispersions along Γ -*X* as in pure GaAs(100), however, shifted by 100–200 meV for large portions of the Δ_1 band. More importantly, the experiments permitted the direct observation of the acceptor states induced by Mn doping near E_F by comparison to pure GaAs spectra for various photon energies also without resonant excitation.⁸

Recently, photoemission spectra have been studied in dependence of the Mn concentration.⁹ Reference 9 obtains a concentration-dependent position of the Mn 3*d* emission from $\text{Ga}_{1-x}\text{Mn}_x\text{As}$ with ~ -3.5 eV for $x=0.045$ and 0.055 . Other spectral features are not reported. In particular, no satellite emission was seen, and it was concluded that local-density theory gives a proper description of the Mn contribution to the spectra.⁹

Magnetic circular x-ray dichroism (MCXD) in absorption at the Mn *L* edge for $\text{Ga}_{1-x}\text{Mn}_x\text{As}$ has been reported^{10,11} and analyzed in comparison to theory.^{11,12} For the number of Mn 3*d* electrons, 5.08 has been obtained¹¹ and a small fraction of ferromagnetically ordered Mn moments among all Mn impurities.

As at the *M* edge, resonant photoemission at the *L* edge can be described as interference between a direct photoemission channel $2p^63d^n \rightarrow 2p^63d^{n-1} + e^-$ and the decay of an excited state $2p^53d^{n+1} \rightarrow 2p^63d^{n-1} + e^-$. Resonant photoemission at the transition-metal *L* edge has been predicted to lead to an enhancement of valence-band photoemission much larger than that at the *M* edge,¹³ and experiments have been performed for compounds^{14,15} and metals¹⁶ but despite its potential the method has not yet been applied to diluted systems, to our knowledge. For the size of the enhancement, values between 10 and 100 have been quoted.¹⁴ It is expected that dilution increases electron correlation and that an enhanced electron correlation will increase the resonant enhancement. Moreover, due to the dilution, we can determine the enhancement precisely via normalization to the core-level intensity of a host constituent. These advantages together with the large size of the enhancement permit a discussion of the 3*d* spectral shape rather independently from the spectrum of the host material. Due to the comparatively large probing depth at kinetic energies around the 2*p* binding energy (≈ 10 Å), the resulting 3*d* contribution is rather independent of the electronic structure of the surface and its quality. The Mn 3*d* contribution determined in this way will be compared to new calculations and to previous experimental results performed at higher surface sensitivity.

II. EXPERIMENTS

Samples were an *n*-type GaAs(100) crystal and a 50-nm-thick epitaxial film of $\text{Ga}_{1-x}\text{Mn}_x\text{As}$, $x=0.043$, grown at 250 °C on top of an $\text{Al}_{0.8}\text{Ga}_{0.2}\text{As}$ buffer layer and subsequently capped with an As cap of ≈ 100 -nm thickness.¹⁷ The sample had a Curie temperature of ≈ 60 K. Decapping and removal of oxidized layers was done with noble-gas ion sputtering monitored by Mn 2*p* photoemission as before.^{5,18} In order to establish a $p(1\times 1)$ low-energy electron-diffraction pattern while avoiding formation of NiAs-type MnAs precipitates, the sample was repeatedly annealed up to 240 °C as maximum. The sample mounting ensured that the GaAs reference sample was heated to the same temperature.

Measurement temperature was 30 K. Synchrotron radiation from the UE56/2 PGM helical undulator beam line¹⁹ was used to excite photoelectrons, namely, linearly polarized light of 62.5 eV and circularly polarized light around the Mn *L* edge (≈ 640 eV). Photoemission spectra were measured with an Escalab MK2 spherical analyzer in normal-emission geometry at 1° angle resolution and 50-meV energy resolution for 62.5-eV photon energy and with angle integration and 0.8-eV resolution for energies around the Mn *L* edge. X-ray absorption spectra were measured with a total-yield channeltron during simultaneous scanning of monochromator and undulator. Base pressure was 2×10^{-10} mbar.

For an overview, Fig. 1 shows resonant photoemission spectra for the $\text{Ga}_{1-x}\text{Mn}_x\text{As}$, $x=0.043$, and pure GaAs as well as the difference spectra representing the Mn 3*d* contribution. The energy range includes the Ga 3*d* core levels and this was used for normalization. The spectra were superimposed precisely taking into account the Ga concentration (100% and 95.7%, respectively). The much stronger enhancement of the Mn 3*d* signal at the Mn *L* edge (640.3 eV) as compared to a photon energy above the Mn *M* edge (62.5 eV) is apparent from the figure. Figure 2 shows the photon-energy dependence more in detail. Photon energies are indicated with the x-ray absorption spectrum in the inset. Below the resonance [Fig. 2(b), 638.5 eV] the Mn 3*d* contribution is negligible whereas on resonance [Fig. 2(c), 640.3 eV] it is dominant. The main peak at -4.3 eV experiences a giant enhancement at the L_3 maximum by a factor of 20 with respect to the pre-edge spectrum (638.5 eV). Besides the main peak, there appears a satellite structure and intensity between the main peak and E_F . Although the satellite seemingly possesses a structure, most likely the dip around -8.5 eV is just intensity that has insufficiently been removed by the subtraction. In addition, the sample has been magnetized by a pulse along the in-plane [010] direction. A sizeable magnetic circular dichroism effect was not observed in the photoemission spectrum at 640.3-eV photon energy after reversing the helicity of the synchrotron radiation. This is in line with the small magnetic circular dichroism effect measured in x-ray absorption.^{10,11} The x-ray absorption line-shape, however, is smoother and deviates more strongly from the atomic d^5 configuration than in Refs. 10 and 11.

Above the L_3 edge, the photoemission intensity is still enhanced, however, the spectral shape is dominated by emission around kinetic energies where LMM Auger contributions are expected. These are marked by an arrow in Fig. 2(d). This intensity can still be distinguished in the L_2 -edge range [Figs. 2(e) and 2(f)].

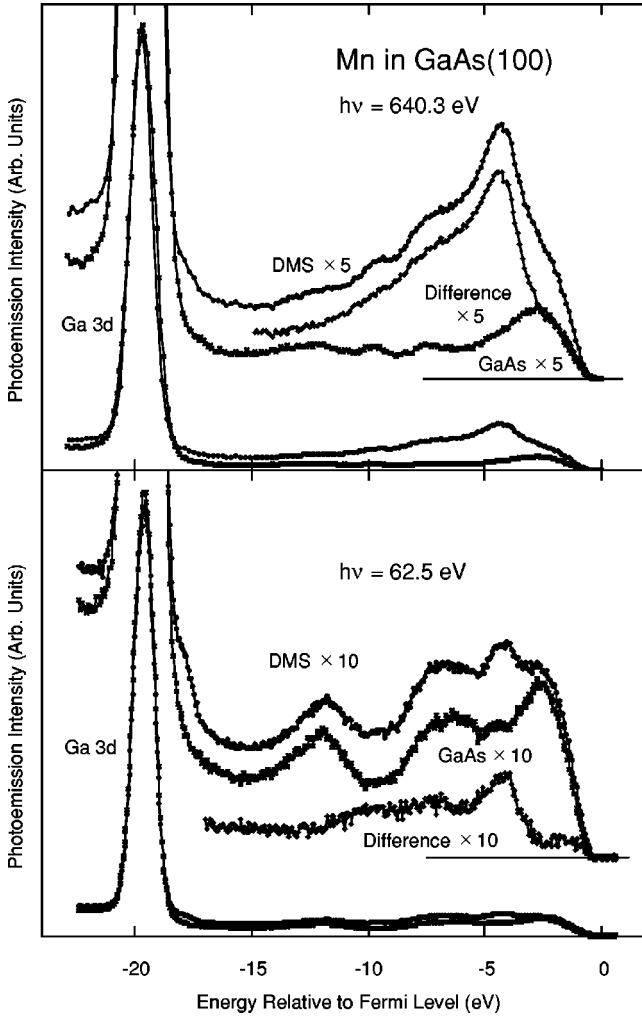


FIG. 1. Resonant photoemission spectra for the diluted magnetic semiconductor (DMS) $\text{Ga}_{1-x}\text{Mn}_x\text{As}(100)$, $x=0.043$, (dots), pure $\text{GaAs}(100)$ (crosses), and the difference between the two (diamonds). The Ga $3d$ core levels have been used for proper normalization of the spectra. The enhancement of the Mn $3d$ contribution (diamonds) at the Mn L edge (b) is much stronger than that above the M edge (a).

To compare to previous experiments, we measured spectra at 62.5-eV photon energy, i.e., above the Mn M edge where the Mn $3d$ contribution is not determined by resonant photoemission but by the enhanced photoemission cross section of Mn $3d$ as compared to Ga and As $4p$. Nevertheless, the enhancement is substantial. In particular in view of the fact that for photon energies between 18 and 40 eV a contribution from the Mn $3d$ main peak cannot be observed at all for a sample with $x=0.035$.⁸ Instead, we see the typical shape of the main peak, satellite and intensity near E_F in the difference spectrum of Fig. 2(a).

III. CALCULATIONS

We have calculated resonant photoemission spectra on the basis of a cluster model with configuration interaction and multiplet splittings. The method has previously been applied

to all $3d$ -transition-metal monoxides in Ref. 13 where a detailed description of the method can be found. In brief, the initial state considers three configurations of the MnAs_4 cluster, i.e.,

$$|i\rangle = \alpha_0|3d^5\rangle + \alpha_1|3d^6\bar{L}\rangle + \alpha_2|3d^7\bar{L}^2\rangle.$$

Here, \bar{L} denotes a ligand hole, which corresponds to the transfer of an electron from an As $4p$ orbital to a Mn d orbital. The charge-transfer energy is defined as $\Delta = E(3d^6\bar{L}) - E(3d^5)$ with $E(3d^6\bar{L})$ and $E(3d^5)$ being the average energies of the $3d^6\bar{L}$ and $3d^5$ configurations, respectively. The $3d$ - $3d$ Coulomb interaction energy is $U_{dd} = E(3d^6) + E(3d^4) - 2E(3d^5)$. The transfer integrals describing the hybridization between Mn $3d$ and As $4p$ are expressed in terms of Slater-Koster parameters ($pd\pi$) and ($pd\sigma$). As usual, the $2p$ - $3d$ Coulomb interaction energy U_{cd} has been tied to U_{dd} by the assumption $U_{dd}/U_{cd} = 0.8$. The intermediate state is given by

$$|m\rangle = \beta_0|2p^53d^6\rangle + \beta_1|2p^53d^7\bar{L}\rangle + \beta_2|2p^53d^8\bar{L}^2\rangle,$$

and the final state of Mn $3d$ photoemission is given by

$$|f\rangle = \gamma_0|3d^4\rangle + \gamma_1|3d^5\bar{L}\rangle + \gamma_2|3d^6\bar{L}^2\rangle.$$

The resonant photoemission spectrum for photon energy ω and photoelectron energy ϵ is expressed as

$$F(\epsilon, \omega) = \sum_f |\langle f\epsilon | T(\omega) | i \rangle|^2 \delta(\omega + E_i - \epsilon - E_f)$$

with initial- and final-state energies E_i and E_f , respectively, $\langle f\epsilon |$ being the direct product of the final state $\langle f |$ of the MnAs_4 cluster and the photoelectron final state $\langle \epsilon |$. The T -matrix $T(\omega)$ includes perturbation operators for the direct dipole transition from $3d$ to ϵl , for the dipole transition from $2p$ to $3d$, and for the Coster-Kronig decay processes from the intermediate state $|m\rangle$.

Figure 3 shows at the top the calculated x-ray absorption spectrum. Capital letters denote photon energies for which resonant photoemission spectra are displayed in the bottom panel. The parameters are the same as those used in Refs. 5 and 6, namely, $\Delta = 1.5$ eV, $(pd\sigma) = 1.0$ eV, and $U_{dd} = 3.5$ eV. The calculation reproduces the x-ray absorption spectrum of Fig. 2 very well apart from the splitting at the L_2 edge which has vanished as compared to previous work.^{10,11} Together with the multiplet lines we show photoemission spectra broadened by a Gaussian of 1.4-eV full width at half maximum. The off-resonance spectrum A shows a strong main peak and strong satellite. Because of $\Delta < U_{dd}$, the main peak is assigned to $3d^5\bar{L}$ and the satellite to $3d^4$ configurations. The on-resonance spectrum C is strongly enhanced but otherwise quite closely resembles the off-resonance spectrum A. The spectral shape does change considerably in the L_3 region, F, and G. It appears as if the relative enhancement of the satellite region with respect to the main peak is rather driven by energy levels in an intermediate energy range (2-eV higher binding energy than the main peak) where mainly $3d^4$ and $3d^6\bar{L}^2$ states contribute.

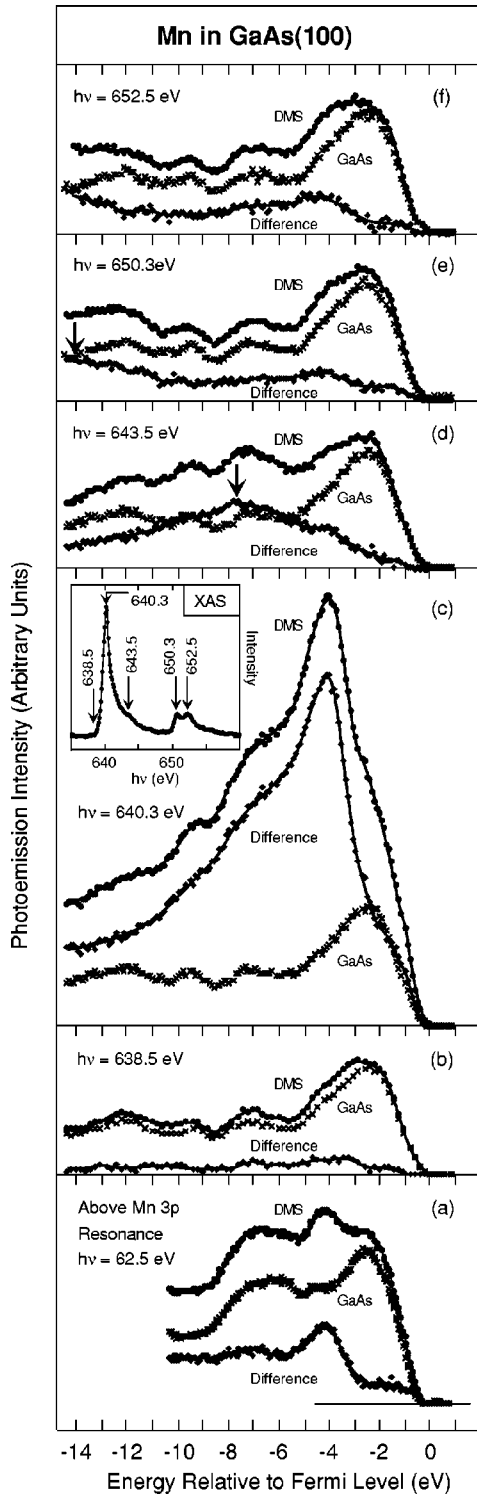


FIG. 2. Resonant photoemission spectra for photon energies above the Mn *M* edge (a) and across the *L* edge (b–f). In addition, the x-ray absorption spectrum is shown in the inset. On resonance (c), the Mn *3d* contribution is 20-fold enhanced but intensity near E_F remains very low.

IV. DISCUSSION

Both experiment, Fig. 2, and theory, Fig. 3, indicate that photoemission spectra at the L_3 edge can very well be used

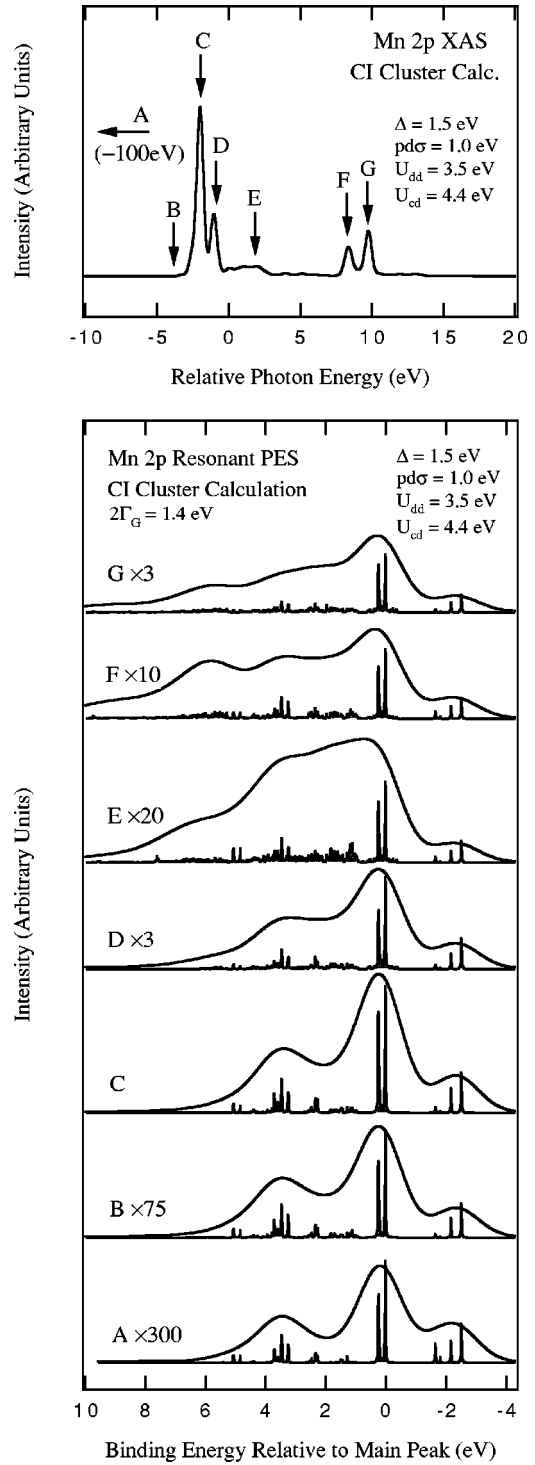


FIG. 3. X-ray absorption (top) and resonant photoemission spectra (bottom) calculated based on a configuration-interaction approach with multiplet splitting for a $MnAs_4$ cluster.

to extract the Mn *3d* spectral weight. Both show that the enhancement is so large that the characteristic features can be appreciated even without the exact subtraction of the host-material spectrum as it was conducted here. We can also estimate from Figs. 2 and 3 that about half of the intensity tentatively assigned to incoherent Auger transitions (arrows in Fig. 2) is, by comparison to spectrum *E* of the calculation,

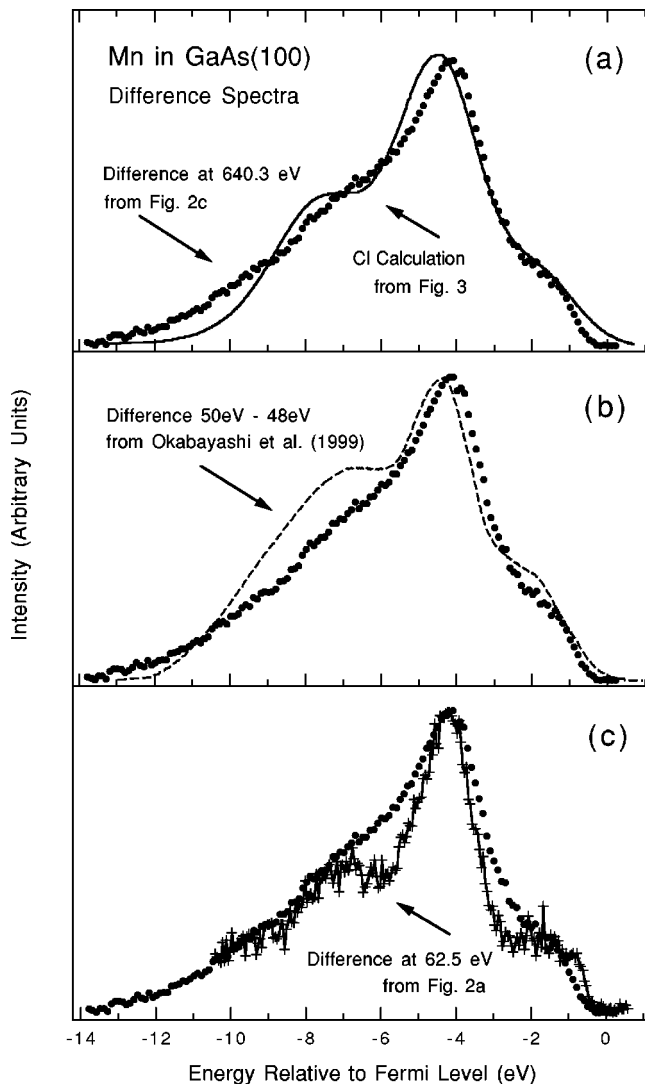


FIG. 4. Comparison of the Mn 3d contribution extracted at 640.3-eV photon energy (dots) to the calculation from Fig. 3 broadened by 2 eV (solid line), to the experimental difference for $\text{Ga}_{1-x}\text{Mn}_x\text{As}$, $x=0.069$ ($h\nu=50$ -eV spectrum minus $h\nu=48$ -eV spectrum), from Ref. 6 (dashed line), and to the one at $h\nu=62.5$ eV from Fig. 2(a) (crosses). An integrated background has been subtracted from each spectrum.

actually due to the resonant photoemission and Auger processes.

The appearance of the satellite structure confirms our previous result^{5,6,8} that local-density theory^{7,20-22} cannot describe the present system in contrast to conclusions from recent photoemission results.⁹ Another shortcoming of local-density theory is that it leads to too high density of states at E_F and too low binding energy of the Mn 3d main peak, at least unless corrections due to the Coulomb interaction are introduced (LDA+ U).²³

We want to further discuss the photoemission spectrum measured at 640.3 eV. Figure 4(a) shows a comparison to the calculated spectrum C but with $2\Gamma_G=2$ eV Gaussian broadening instead of 1.4 eV. It should be noted that the broad shape is not caused by the experimental resolution (which

has directly been measured from molybdenum clamps in contact with the sample). Instead, incoherent Auger contributions, the finite width of the host valence band, and electron-phonon interaction are possible sources of the strong broadening. Among these, electron-phonon interaction will be limited by the total width of 1.25 eV measured from the Ga 3d core levels displayed in Fig. 1. We believe that the width of the GaAs valence band is the main source of the broadening. For $\text{Cd}_{1-x}\text{Mn}_x\text{Te}$, the Andersen impurity model has been applied,²⁴ and a Mn 3d density of states has been obtained that is similar to the configuration-interaction cluster model²⁵ but with broad spectral features.

Figure 4(b) compares the new data to the M -edge resonant photoemission of $\text{Ga}_{1-x}\text{Mn}_x\text{As}$, $x=0.069$ (Ref. 6). The spectra are very similar but the intensity of the satellite is higher when measured at 50-eV photon energy, and the higher intensity has very well been reproduced by the configuration-interaction calculation in Ref. 6 for a parameter set identical to the present one. This deviation was already noted for NiAs-type MnTe where the Mn 3d satellite intensity is also weaker as compared to the main peak for L -edge than for M -edge resonant photoemission experiments.¹⁵

Finally, we superimpose in Fig. 4(c) the 62.5-eV difference spectrum for the same $\text{Ga}_{1-x}\text{Mn}_x\text{As}$, $x=0.043$, sample. The difference spectrum at this photon energy is determined by enhanced Mn 3d photoionization cross section instead of resonant Mn M -edge photoemission, and the photon energy is high enough to keep Auger transitions out of the energy range of interest. Obviously, at this energy the determination of the difference spectrum is more sensitive to GaAs subtraction than for resonant photoemission at the L edge because the enhancement is smaller, band-structure effects are stronger, and surface effects can contribute more strongly. Details of the annealing procedure may therefore matter much more. Note that difference spectra at 70-eV photon energy have led to extra structure around -2 eV and even to negative intensities.⁶ This could be due to surface states as well as Mn-induced shifts of the bulk GaAs valence bands as established for the Δ_1 band.⁸ These are reasonable causes since the difference between 50- and 48-eV photon-energy spectra from the same sample as studied at 70 eV is completely positive.⁸ The surface sensitivity (which is very similar at 50 and 70 eV) is, therefore, a matter of the GaAs host. Taking this into account, the fact that the present difference spectrum at 62.5 eV gives a rather good rendering of the Mn 3d contribution indicates that choice of the photon energy indeed influences the results through the corresponding direct transitions of surface and bulk states of the GaAs host and that there is no indication for a particular surface dependence of the Mn 3d contribution itself.

The 62.5-eV spectrum and the 640.3-eV spectrum agree with respect to their extremely weak intensity at E_F [Fig. 4(c)]. Although the intensity of the 62.5-eV spectrum rises much steeper, the intensity becomes very weak at the same energy (about -0.3 eV). The low intensity at E_F rules out a strong Mn 3d contribution there. This means also that while $\text{Ga}_{1-x}\text{Mn}_x\text{As}$ may be a half metal as suggested in Ref. 7, the half metallicity cannot result from Mn 3d states as obtained

in Ref. 7. Half metallicity may result instead from full polarization of As $4p$ states by interaction with Mn $3d$. On the other hand, this result confirms the importance of As $4p$ holes as mediators of the magnetic coupling.

An expectation connected to resonant photoemission at the L edge is sensitivity to the electron configuration. Resonant photoemission at the L -edge of CuO (Ref. 14) is a particular example since the decay channel can principally enhance $3d^8$ through $3d^9 + h\nu \rightarrow 2p^5 3d^{10} \rightarrow 2p^6 3d^8 + e^-$ but not $3d^9 \underline{L}$ final states since a corresponding channel does not exist. In the present case of Mn^{2+} , both $3d^5 + h\nu \rightarrow 2p^5 3d^6 \rightarrow 2p^6 3d^4 + e^-$ and $3d^6 L + h\nu \rightarrow 2p^5 3d^7 \underline{L} \rightarrow 2p^6 3d^5 \underline{L} + e^-$ exist and have similar matrix elements and transition probabilities. Therefore, on- and off-resonance spectra ($A-C$) are very similar to each other in Fig. 3.

We have to caution that our analysis based on the configuration-interaction scheme is limited by the assumption of identical Mn sites. Although the reason for the different x-ray absorption lineshape has not yet been established, MCXD data indicate that the ferromagnetically ordered portion of Mn atoms is small.^{10,11} Spin-resolved photoemission would give the $3d$ density of states of the ferromagnetically aligned Mn atoms. In resonant photoemission at the Mn M edge, the spin polarization was too small to extract a density of states.²⁶ Mn L -edge resonant photoemission with its high intensity and small GaAs host signal is possibly better suited for spin-resolved studies.

Finally, we want to briefly return to the probing depth. It was recently argued that photoemission data obtained at photon energies in the vacuum-ultraviolet range cannot probe bulk properties and that energies in the soft-x-ray region need to be used.²⁷ According to this view, the resonant valence-band photoemission at the L edge would probe bulk properties while the one at the M edge does not. Consequently, parameters deduced from the Mn $2p$ core level measured at ≈ 600 -eV kinetic energy⁵ represent the bulk whereas those from resonant valence-band photoemission⁶ at the Mn M edge and above it (kinetic energies between 45 eV and 65

eV) do not. The present study confirms the conclusions and the values of the parameters Δ , U_{dd} , and $(pd\sigma)$ from both previous studies and reassures that the reduced probing depth of resonant photoemission at the Mn M edge does not affect the conclusions. This is likely to be connected to the careful surface preparation exercised but is also due to the dilution. The applicability of the cluster model emphasizes the importance of nearest-neighbor atoms. As long as Mn remains on substitutional lattice sites and does not segregate to the top-most atomic layer, its electronic structure will remain largely the same. On the other hand, segregation of Ga or As would not affect our results very much as Mn atoms from deeper inside the bulk would still contribute to our difference spectra. In this case, the probing depth of the Mn $3d$ signal would even increase.

V. CONCLUSIONS

We studied resonant photoemission of $p(1 \times 1)$ $\text{Ga}_{1-x}\text{Mn}_x\text{As}(100)$, $x=0.043$, and $p(1 \times 1)$ $\text{GaAs}(100)$ at photon energies above the Mn M edge and through the Mn L edge. The huge enhancement at the L edge ($\sim \times 20$) facilitates the extraction of the Mn $3d$ spectral contribution which is characterized by a three-peak structure including an intense correlation satellite. The x-ray absorption and resonant photoemission spectra are well described by a calculation using configuration interaction with multiplet splitting on a MnAs_4 cluster model. Experiment and model calculations agree with our previous work at the M -edge and are at variance with x-ray absorption and with recent photoemission results which obtained no satellite and suggested a description by an itinerant model.

ACKNOWLEDGMENT

This work was supported by BMBF under Contract No. 05 KS11PA/0 and by a Grant-in-Aid for Scientific Research in Priority Area ‘‘Semiconductor Spintronics’’ (Contract No. 14076209) from MEXT, Japan.

*Electronic address: rader@bessy.de

[†]Permanent address: Institute of Physics, St. Petersburg State University, Uljanovskaja 1, Petrodvoretz, St. Petersburg 198504, Russia.

¹H. Munekata, H. Ohno, S. von Molnár, A. Segmüller, L.L. Chang, and L. Esaki, Phys. Rev. Lett. **63**, 1849 (1989).

²H. Ohno, H. Munekata, T. Penney, S. von Molnár, and L.L. Chang, Phys. Rev. Lett. **68**, 2664 (1992).

³H. Ohno, A. Shen, F. Matsukura, A. Oiwa, A. Endo, S. Katsumoto, and Y. Iye, Appl. Phys. Lett. **69**, 363 (1996).

⁴H. Ohno, Science **281**, 951 (1998).

⁵J. Okabayashi, A. Kimura, O. Rader, T. Mizokawa, A. Fujimori, T. Hayashi, and M. Tanaka, Phys. Rev. B **58**, R4211 (1998).

⁶J. Okabayashi, A. Kimura, T. Mizokawa, A. Fujimori, T. Hayashi, and M. Tanaka, Phys. Rev. B **59**, R2486 (1999).

⁷H. Akai, Phys. Rev. Lett. **81**, 3002 (1998).

⁸J. Okabayashi, A. Kimura, O. Rader, T. Mizokawa, A. Fujimori, T. Hayashi, and M. Tanaka, Physica E (Amsterdam) **10**, 192

(2001); Phys. Rev. B **64**, 125304 (2001).

⁹H. Åsklund, L. Ilver, J. Kanski, J. Sadowski, and R. Mathieu, Phys. Rev. B **66**, 115319 (2002).

¹⁰H. Ohldag, V. Solinas, F.U. Hillebrecht, J.B. Goedkoop, M. Finazzi, F. Matsukura, and H. Ohno, Appl. Phys. Lett. **76**, 2928 (2000).

¹¹S. Ueda, S. Imada, T. Muro, Y. Saitoh, S. Suga, F. Matsukura, and H. Ohno, Physica E (Amsterdam) **10**, 210 (2001).

¹²G. van der Laan and B.T. Thole, Phys. Rev. B **43**, 13 401 (1991).

¹³A. Tanaka and T. Jo, J. Phys. Soc. Jpn. **63**, 2788 (1994).

¹⁴L.H. Tjeng, C.T. Chen, J. Ghijsen, P. Rudolf, and F. Sette, Phys. Rev. Lett. **67**, 501 (1991).

¹⁵H. Sato, A. Tanaka, A. Furuta, S. Senba, H. Okuda, K. Mimura, M. Nakatake, Y. Ueda, M. Taniguchi, and T. Jo, J. Phys. Soc. Jpn. **68**, 2132 (1999).

¹⁶M. Weinelt, A. Nilsson, M. Magnuson, T. Wiell, N. Wassdahl, O. Karis, A. Föhlisch, N. Martensson, J. Stöhr, and M. Samant, Phys. Rev. Lett. **78**, 967 (1997).

- ¹⁷T. Hayashi, M. Tanaka, T. Nishinaga, H. Shimada, H. Tsuchiya, and Y. Otuka, *J. Cryst. Growth* **175/176**, 1063 (1997).
- ¹⁸O. Rader, A. Kimura, N. Kamakura, K.-S. An, S. Miyanishi, H. Akinaga, M. Shirai, K. Shimada, and A. Fujimori, *J. Electron Spectrosc. Relat. Phenom.* **88**, 225 (1998).
- ¹⁹M.R. Weiss, R. Follath, K.J.S. Sawhney, F. Senf, J. Bahrtdt, W. Frentrop, H. Gaupp, S. Sasaki, M. Scheer, H.-C. Mertins, D. Abramsohn, F. Schäfers, W. Kuch, and W. Mahler, *Nucl. Instrum. Methods Phys. Res. A* **467-468**, 449 (2001).
- ²⁰M. Shirai, T. Ogawa, I. Kitagawa, and N. Suzuki, *J. Magn. Magn. Mater.* **177-181**, 1383 (1998).
- ²¹S. Sanvito and N.A. Hill, *Phys. Rev. B* **62**, 15 553 (2000); S. Sanvito, P. Ordejon, and N.A. Hill, *ibid.* **63**, 165206 (2001).
- ²²M. van Schilfgaarde and O.N. Mryasov, *Phys. Rev. B* **63**, 233205 (2001).
- ²³J.H. Park, S.K. Kwon, and B.I. Min, *Physica B* **281-282**, 703 (2000).
- ²⁴O. Gunnarsson, O.K. Andersen, O. Jepsen, and J. Zaanen, *Phys. Rev. B* **39**, 1708 (1989).
- ²⁵L. Ley, M. Taniguchi, J. Ghijsen, R.L. Johnson, and A. Fujimori, *Phys. Rev. B* **35**, 2839 (1987).
- ²⁶O. Rader, J. Okabayashi, K. Maiti, and C. Carbone (unpublished).
- ²⁷A. Sekiyama, T. Iwasaki, K. Matsuda, Y. Saitoh, Y. Onuki, and S. Suga, *Nature (London)* **403**, 396 (2000).